35th Annual International Conference of the IEEE EMBS
Osaka, Japan, 3 - 7 July, 2013

Ambulatory Respiratory Rate Detection using ECG and a Triaxial Accelerometer

Alexander M. Chan*, Nima Ferdosi, and Ravi Narasimhan

Abstract— **Continuous monitoring of respiratory rate in ambulatory conditions has widespread applications for screening of respiratory diseases and remote patient monitoring. Unfortunately, minimally obtrusive techniques often suffer from low accuracy. In this paper, we describe an algorithm with low computational complexity for combining multiple respiratory measurements to estimate breathing rate from an unobtrusive chest patch sensor. Respiratory rates derived from the respiratory sinus arrhythmia (RSA) and modulation of the QRS amplitude of electrocardiography (ECG) are combined with a respiratory rate derived from tri-axial accelerometer data. The three respiration rates are combined by a weighted average using weights based on quality metrics for each signal. The algorithm was evaluated on 15 elderly subjects who performed spontaneous and metronome breathing as well as a variety of activities of daily living (ADLs). When compared to a reference device, the mean absolute error was 1.02 breaths per minute (BrPM) during metronome breathing, 1.67 BrPM during spontaneous breathing, and 2.03 BrPM during ADLs.**

I. INTRODUCTION

Accurate estimation of respiratory rate in ambulatory settings is challenging because of inherent limitations of different respiratory measurements. The most reliable techniques tend to be obtrusive: flow measurements require a nasal cannula, respiratory inductance pneumography requires circumferential chest bands, and impedance plethysmography requires electrodes on distant sites on the body. On the other hand, sensors and measurements that are less obtrusive are often more sensitive to noise.

As a result of the miniaturization of microelectromechanical systems-based accelerometers and electrocardiographic (ECG) monitoring devices, methods using ECG-derived respiration and chest-mounted accelerometers can potentially monitor respiration in a minimally obtrusive fashion. Previous studies have demonstrated that respiratory rate can be estimated from ECG signals by examining either the respiratory sinus arrhythmia (RSA) that causes a modulation of R-R intervals (time between consecutive ECG R-waves) during the respiratory cycle [1], or the change of cardiac axis during breathing that manifests itself as a change in QRS amplitude [2, 3]. The use of accelerometers for measuring chest movement during respiration has been relatively less explored; however, the feasibility of accelerometer-based respiration measurement has been demonstrated [4].

Each of these techniques has inherent limitations, but utilizing a combination of these measures may allow for more robust respiratory rate estimation by making up for the specific weaknesses of each method. While ECG-derived respiration is limited to detecting breathing rates of less than one half of the heart rate due to cardiac aliasing [5], accelerometry has no such limitation. Furthermore, while accelerometry can be overwhelmed by noise during periods of ambulation, ECG-derived measures are less sensitive to movement. Finally, while the RSA depends on the functioning of the autonomic nervous system (ANS) and, therefore, decreases with age [6] or particular diseases, QRS-amplitude modulation is caused by mechanical movement of the heart and is unaffected by the ANS [3].

In this study, we demonstrate that by generating a quality metric for each component respiratory signal, a weighting of the component respiratory rate estimates can be computed such that the *combined* respiratory rate estimate is robust in different populations under a variety of conditions. Furthermore, this respiratory rate algorithm is computationally efficient for implementation on a low-power device.

II. METHODS

A. Experimental design

A patch sensor device designed by Vital Connect, Inc. (Campbell, CA) was used to collect simultaneous ECG and accelerometer data. The device acquires a single-lead bipolar ECG sampled at 125 Hz using two electrodes covered with hydrogel discs. A tri-axial accelerometer is also present on the device; the accelerometer has a range of $\pm$4g (where g = 9.81 m/s^2) with a resolution of 0.0078g and is sampled at 62.5 Hz. These data are streamed via Bluetooth low energy (BLE) to a smartphone for storage. The patch device utilizes a coin-cell battery and is adhered to the chest in one of three locations: (1) in a modified lead-II configuration over the 2nd intercostal space (ICS) at the left mid-clavicular line, (2) vertically over the sternum, or (3) horizontally at the 6th or 7th ICS at the left mid-clavicular line. Further information regarding the patch sensor can be found in [7].

The device automatically performs calibration of the accelerometer to obtain vertical (y-axis), antero-posterior (z-axis), and left-right lateral (x-axis) directions during an initial period of standing upright. The respiration algorithms described below were implemented on the embedded processor of the patch sensor, and the respiratory rates were transmitted via an encrypted BLE link to the receiving smartphone.

A total of 15 elderly subjects (7 male, 8 female) between the ages of 63 and 79 (70$\pm$5 years), with height between 147 cm and 185 cm (167$\pm$11 cm) and body mass between 44.7 kg and 99.2 kg (69.4$\pm$14.8 kg) participated in the study. The study consisted of two blocks: one block of spontaneous and metronome breathing while the subject was seated, and

Authors are with Vital Connect Inc., Campbell, CA 95008, USA. (*corresponding author's e-mail: achan@vitalconnect.com)

978-1-4577-0216-7/13/$26.00 ©2013 IEEE

one block of activities of daily living (ADLs). During the first block, the subject performed spontaneous breathing for 4 minutes, followed by 5 blocks of visually-guided metronome breathing at 12, 15, 18, 21, and 24 breaths per minute (BrPM) for 3 minutes each. During the second block of 20 minutes, subjects performed a variety of ADLs including sitting, standing, lying, and walking.

Concurrent with recording of ECG and accelerometer data from the patch sensor, respiratory rate was recorded using an Oridion Capnostream 20 capnography monitor. This device utilizes a nasal cannula to measure end-tidal CO_2 and derive the breathing rate.

B. ECG-derived respiration signals

The RSA is a modulation of the heart rate over the period of a respiratory cycle. Because of the ANS, the heart rate increases on inspiration (R-R intervals decrease) and decreases on expiration (R-R intervals increase); thus the R-R interval series can be utilized as a respiration signal. A wavelet algorithm is utilized to detect R peaks in the ECG [8], and the time between R peaks is taken as the R-R interval series. Because QRS complexes are not regularly spaced, the R-R interval series is resampled to 4 Hz using linear interpolation and low-pass filtered to 0.7 Hz. The sampling rate of 4 Hz is sufficient for the bandwidth of the respiratory signals. This process extracts information in the respiratory frequency range, assumed to be between 0.1 Hz and 0.7 Hz (6 to 42 breaths per minute).

During respiration, the movement of the chest wall imparts motion to the heart and changes the apparent cardiac axis during the respiratory cycle. This change in cardiac axis manifests itself as a modulation of the amplitude of the QRS complex. While previous studies have utilized multi-lead ECG to estimate the cardiac axis directly [3], a similar respiratory signal can be obtained from a single-lead ECG [2]. After R-peak detection, the maximum and minimum ECG values (V_{max} and V_{min}) in a 100 ms window surrounding the R peak (50 ms on each side) are found, and the QRS-amplitude is measured as $V_{max} - V_{min}$. The QRS amplitude measurements are also low-pass filtered to 0.7 Hz and resampled to 4 Hz.

C. Accelerometer signal

Although chest movement during respiration is small, these movements can be detected as a change in the angle θ between the gravitational acceleration vector $\vec{g}$ (where $\vec{g}$ is normalized such that $\|\vec{g}\| = 1$) and a unit vector $\vec{u}$. The best unit vector $\vec{u}$ is nearly perpendicular to $\vec{g}$ ($\theta = 90°$) since, in this case, for a change in angle of $\Delta\theta$, where $\Delta\theta \approx 0$, the component of gravity in the direction $\vec{u}+\vec{\Delta u}$ is $\left(\vec{u}+\vec{\Delta u}\right) \cdot \vec{g}/\|\vec{u}+\vec{\Delta u}\| = \sin(\Delta\theta) \approx \Delta\theta$. Empirically, it was found that for an accelerometer mounted to the anterior surface of the chest, the antero-posterior axis (z-axis) provides the most robust respiration signal while upright or lying in a left or right lateral position while the inferior-superior axis (y-axis) is most informative when supine or prone. To satisfy these conditions, the accelerometer axis used for respiration was computed as,

$$\vec{u} = \frac{\vec{g}}{C} \times \begin{bmatrix} \sin\theta_x \\ \cos\theta_x \\ 0 \end{bmatrix} = \frac{\vec{g}}{C} \times \begin{bmatrix} \sqrt{1-(\vec{g}\cdot\vec{i})^2} \\ \vec{g}\cdot\vec{i} \\ 0 \end{bmatrix} \quad (1)$$

where $C = \|\vec{g} \times [\sin\theta_x \;\; \cos\theta_x \;\; 0]^T\|$, $\vec{i}$ is a unit vector along the x-axis, and $\vec{g}$ is obtained by filtering the raw acceleration components using 2-stage elliptical low-pass biquad filters with a passband corner frequency of 0.01 Hz, stopband corner frequency of 0.02 Hz, 30-dB stopband attenuation and 1-dB passband ripple. The quantity θ_x is the angle of the gravity vector from the x-axis (lateral left-right axis) such that 90° is standing vertically, and 0° is lying in a right-lateral position. Equation (1) simplifies to:

$$\vec{u} = \frac{\vec{g}}{C} \times \begin{bmatrix} \sqrt{1-g_x^2} \\ g_x \\ 0 \end{bmatrix} = \begin{bmatrix} -g_x g_z \\ g_z\sqrt{1-g_x^2} \\ g_x^2 - g_y\sqrt{1-g_x^2} \end{bmatrix} /C \quad (2)$$

To obtain the full respiration signal, the raw accelerometer data are filtered using 3-stage elliptical lowpass biquad filters with a passband corner frequency of 0.7 Hz, a passband ripple of 1 dB, a stopband corner frequency of 0.9 Hz, and a 30-dB stopband attenuation. The filtered acceleration vector is then projected onto the respiration axis, $\vec{u}$, and resampled to 4 Hz to obtain the final respiration signal.

D. Peak-picking and respiratory rate estimation

Respiratory rate was estimated from the respiration signals after a peak-picking algorithm was performed to detect individual breaths. The peak-picking algorithm requires that all maxima be greater than adjacent minima by a threshold that is a multiple, α, of the standard deviation, $\sigma[n]$, of the past M seconds of the respiratory signal. If a local maximum is detected that is greater than the previous candidate maximum and is greater than the current candidate minimum by the threshold $\alpha\sigma[n]$, then this local maximum is assigned as the new candidate maximum. If a local minimum is detected that is less than the candidate maximum by the threshold $\alpha\sigma[n]$, then the candidate local maximum becomes a true maximum, the candidate left minimum becomes a true minimum, and the current minimum is updated as the candidate left minimum. If the local minimum is not less than the candidate maximum by the threshold $\alpha\sigma[n]$, but is less than the current candidate left minimum, the local minimum becomes the candidate left minimum.

This peak-picking algorithm is insensitive to large DC offsets that may be present in the accelerometer-based respiration signal, and the variable peak-sensitivity (based on the local standard deviation) makes the algorithm robust to extraneous peaks caused by noise. The peak-picking parameters are set to M=3 seconds and α=1.1 for the accelerometer-based respiration signal, M=3 seconds and α=0.65 for the RSA signal, and M=4 seconds and α=0.75 for the QRS-amplitude signal.

To estimate the respiratory rate from the picked peaks, the times between successive maxima are computed for a

45-second window, shifted every 5 seconds, and the instantaneous breathing rates are calculated. The mean breathing rate is computed after the top 10% and bottom 10% of instantaneous breathing rates are discarded. A linear correction is applied to each respiration rate to correct for proportional biases using the equation $\text{BR}_{\text{unbiased}} = m * \text{BR} + b$, where BR denotes breathing rate and m and b are correction factors. The corrections used were m_{RSA}=1.15, m_{QRSa}=1.15, m_{accel}=1.05, b_{RSA}=-2, b_{QRSa}= -2, and b_{accel}=0 where the subscripts "RSA", "QRSa" and "accel" correspond to the respiratory signals from RSA, QRS amplitude and accelerometer data, respectively, and were determined by linear regression.

E. Quality metric and weighting

While the above algorithms generate a separate breathing rate for each of the respiratory signals, a method is needed to combine the estimated rates depending on the quality of the underlying signals. To this end, a quality metric, Q, ranging from 0 to 1, is computed for each respiratory signal to denote the reliability of the estimated rate from that signal. The final breathing rate is computed as the weighted mean of the breathing rates from all signals:

$$\text{BR}_{\text{combined}} = \frac{Q_{\text{RSA}}\text{BR}_{\text{RSA}} + Q_{\text{QRSa}}\text{BR}_{\text{QRSa}} + Q_{\text{accel}}\text{BR}_{\text{accel}}}{Q_{\text{RSA}} + Q_{\text{QRSa}} + Q_{\text{accel}}}. \quad (3)$$

Furthermore, because ECG-derived respiration is limited to detecting breathing rates of less than half the heart rate (cardiac aliasing), the algorithm relies on the accelerometer-based breathing rate when it is of good quality. Thus, if $Q_{\text{accel}} > T$ and $\text{BR}_{\text{accel}} > \frac{\text{HR}}{2}$, where HR denotes the current heart rate estimate, then $Q_{\text{RSA}} = 0$ and $Q_{\text{QRSa}} = 0$. In this case, $T = 0.8$.

Derivation of the quality metric for each respiratory signal utilizes a linear weighting of four features computed during the peak-picking algorithm. These features, which are computed for a given 45-second window, are (1) the coefficient of variation (standard deviation divided by the mean) of peak-to-peak amplitudes, (2) the mean peak-to-peak amplitude, (3) the coefficient of variation of the time between successive minima, and (4) the ratio of the number of true maxima and minima to all local maxima and minima. These features provide a measure of the regularity of the peaks of the respiration signal such that the more regular the peaks, the more likely these peaks truly reflect respiration. An estimate of the breathing rate error, $\hat{E}$, is computed as a linear combination of the four features, $\hat{E} = \max(0, \alpha_1 f_1 + \alpha_2 f_2 + \alpha_3 f_3 + \alpha_4 f_4 + \alpha_5)$, and the coefficients, α_i, are learned using least squares regression on an independent training dataset of 24 subjects. The estimated error is converted to a quality measure using $Q = e^{-\hat{E}/\tau}$ which ranges from 0 (for low quality) to 1 (for high quality), where τ is a constant that determines the correspondence between the estimated error and the quality metric. The constant is empirically set to $\tau = 5$, which equates a 1 BrPM error to a quality of approximately 0.8. If the amplitude of the respiration signal is small (i.e. close to noise), the quality is reduced as follows: if the mean peak-to-peak amplitude, f_2, is below some threshold, P, the quality is multiplied by $\frac{f_2}{P}$. In this case, P is set to 50 ms for the RSA algorithm, 100 μV for the QRS-amplitude algorithm, and 0.01g for the accelerometer algorithm.

TABLE I

MEAN AND STANDARD ERRORS OF MAE AND RMSE ACROSS SUBJECTS

Location	Metronome	Spontaneous	ADLs
Mean Absolute Error (BrPM)			
1	1.02±0.07	1.70±0.09	2.09±0.10
2	1.09±0.11	1.73±0.10	2.02±0.07
3	0.96±0.10	1.58±0.08	1.97±0.08
Root-mean-square Error (BrPM)			
1	1.57±0.23	3.71±0.36	5.65±0.48
2	2.17±0.42	4.87±0.68	7.26±0.85
3	1.65±0.36	3.16±0.30	5.09±0.40

III. RESULTS

Data from 5 patches (out of a total of 45) were excluded from analysis because of poor ECG quality caused by a lack of adequate electrode-to-skin contact (e.g., from interference of chest hair). To assess the accuracy of the algorithm presented above, the last minute of each metronome breathing block was extracted and the mean absolute error (MAE) and root mean squared error (RMSE) were computed between the patch-derived combined respiratory rate and the capnography-derived (reference) respiratory rate. These errors were also computed for the 4-minute spontaneous breathing block as well as during the activities of daily living (ADLs). These results are presented in Fig. 1 and Table I. While all three locations demonstrate very similar errors, the errors from Location 3 were generally smaller than the errors at the other two sites.

On average, the combined respiration rate demonstrated lower MAE than each of the component rates during metronome breathing (Fig. 2). Compared to the combined rate, the MAE was, on average, 0.39, 0.15, and 0.27 BrPM

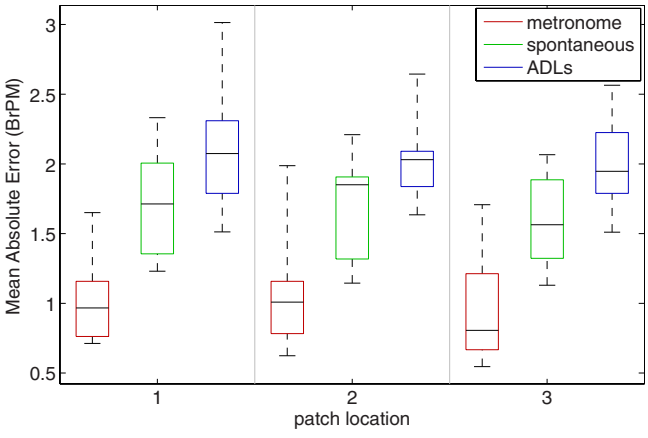

Fig. 1. Box and whisker plots of the mean absolute error (MAE) of respiratory rate at each of the three sensor locations during metronome breathing, spontaneous breathing, and ADLs. The black horizontal line indicates the median, the box indicates the 25^{th} and 75^{th} percentiles, and the whiskers indicate the extreme values.

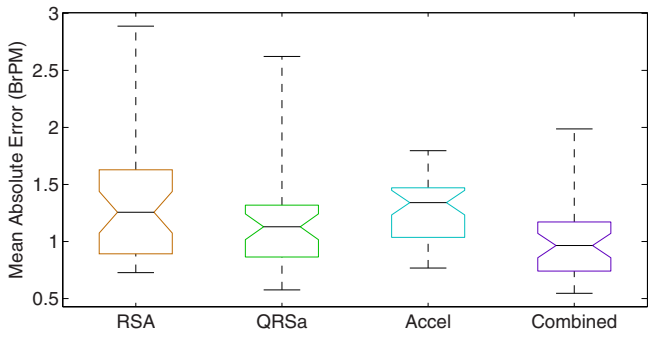

Fig. 2. Box and whisker plots of the mean absolute error (MAE) of the respiratory rates from the individual signals (RSA, QRS amplitude, accelerometry) as well as the combined respiratory rate. Notches indicate 95% confidence intervals of the medians.

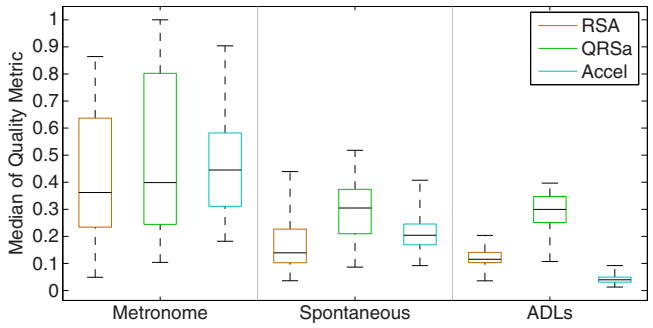

Fig. 3. Box plots of the median quality metrics of the individual respiratory signals (RSA, QRS amplitude, accelerometry) during metronome breathing, spontaneous breathing, and ADLs

greater for RSA, QRS-amplitude, and accelerometer-based respiratory rates, respectively ($p < 0.01$, paired t-test). The results demonstrate, as expected, that the combined respiratory rate significantly improves accuracy over any single respiratory signal alone.

Examination of median quality metrics showed similar quality of all three signals during metronome breathing (Fig. 3). During spontaneous breathing and ADLs, all qualities dropped, but QRS-amplitude was the least affected. As expected, accelerometer quality suffered the most during ADLs due to large body movements. Similarly, abrupt changes in heart rate during ADLs also adversely affected RSA quality.

Bland-Altman analysis of the patch-derived combined respiration rate compared with capnography for metronome breathing yielded a mean bias of -0.29 BrPM, and limits of agreement at -4.41 BrPM and 3.82 BrPM (Fig. 4).

IV. CONCLUSIONS

While unobtrusive indirect respiratory signals are often noisy, utilizing a weighted combination of measurements allows for the robust estimation of the respiratory rate from ECG and a tri-axial accelerometer in a chest patch sensor. This method allows for the combination of any number of additional respiratory signals, such as impedance pneumography, chest bands, or flow measurements. The use of a quality metric to characterize each of the individual components allows the final estimated respiration rate to rely on the

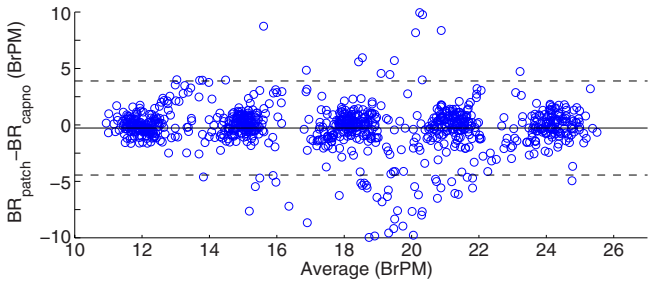

Fig. 4. Bland-Altman plot of the respiratory rates from capnography and from the patch sensor for metronome breathing. The bias is shown as a solid black line (-0.29 BrPM). Limits of agreement are shown as dashed lines (-4.41 to 3.82 BrPM).

signals that are most reliable in any particular situation. The results shown here demonstrate that all three patch locations are equivalent in terms of error, and can be used to measure respiration. The relatively low complexity of the algorithm allows it to be implemented on an embedded processor in the patch sensor used in this study.

This paper presented a method that combines a set of respiratory *rates* that are derived from individual respiratory *signals*; however, it may be possible to combine the respiratory signals themselves even when the quality of the signals is variable. This approach may improve the measurement of other respiratory features apart from rate (e.g., respiratory effort and variability in breathing) that are useful in screening and diagnosing a variety of respiratory conditions.

ACKNOWLEDGMENT

The authors thank the Cardiac Therapy Foundation (Palo Alto, CA) for providing the testing facility and assisting in recruitment of participants, and N. Selvaraj, L. Pham, S. Mostafavi, and L. DeMoss for help with organizing and conducting many aspects of the field trial.

REFERENCES

[1] E. J. C. de Geus, G. H. M. Willemsen, C. H. A. M. Klaver, and L. J. P. van Doornen, "Ambulatory measurement of respiratory sinus arrhythmia and respiration rate," *Biological Psychology*, vol. 41, no. 3, pp. 205–227, 1995.

[2] Y. Zhao, J. Zhao, and Q. Li, "Derivation of respiratory signals from single-lead ecg," in *Future BioMedical Information Engineering, International Seminar on*, 2008, pp. 15–18.

[3] G. B. Moody, R. G. Mark, A. Zoccola, and S. Mantero, "Derivation of respiratory signals from multi-lead ecgs," *Computers in Cardiology*, vol. 12, pp. 113–116, 1985.

[4] P. D. Hung, S. Bonnet, R. Guillemaud, E. Castelli, and P. T. N. Yen, "Estimation of respiratory waveform using an accelerometer," in *Biomedical Imaging, IEEE International Symposium on*, 2008, pp. 1493–1496.

[5] H. Witte, U. Zwiener, M. Rother, and S. Glaser, "Evidence of a previously undescribed form of respiratory sinus arrhythmia (rsa) — the physiological manifestation of "cardiac aliasing"," *Pflügers Archiv Eur. J. of Physiol.*, vol. 412, pp. 442–444, 1988.

[6] J. B. Hellman and R. W. Stacy, "Variation of respiratory sinus arrhythmia with age," *J. of Appl. Physiol.*, vol. 41, no. 5, pp. 734–738, 1976.

[7] A. M. Chan, N. Selvaraj, N. Ferdosi, and R. Narasimhan, "Wireless patch sensor for remote monitoring of heart rate, respiration, activity, and falls," *Eng. in Med. and Biol. Society, Conf. of the IEEE*, 2013.

[8] C. Li, C. Zheng, and C. Tai, "Detection of ecg characteristic points using wavelet transforms," *Biomedical Engineering, IEEE Transactions on*, vol. 42, no. 1, pp. 21–28, 1995.